

# On the Performance of MIMO Full-Duplex Relaying System With SWIPT Under Outdated CSI

Tran Manh Hoang , Xuan Nam Tran , *Member, IEEE*, Ba Cao Nguyen , and Le The Dung , *Member, IEEE*

**Abstract**—In this paper, we propose a full-duplex (FD) relaying system with multi-input multi-output (MIMO) with simultaneous wireless information and power transfer (SWIPT), where the communication from source to destination is assisted by a full-duplex decode-and-forward (DF) relay. The time switching (TS) protocol is used at the relay to harvest the energy of radio-frequency (RF) signals transmitted from the source. To improve both system performance and the amount of harvested energy, multiple antennas are used at source and destination. Transmit antenna selection (TAS) is employed at the source with an assumption that the feedback of channel state information (CSI) is outdated. Meanwhile, both selection combining (SC) and maximal ratio combining (MRC) techniques are applied at the destination. The closed-form expressions of the outage probability (OP), optimal throughput, and symbol error probability (SEP) are derived subject to the outdated CSI over Rayleigh fading channels. We also make a comparison between the performance of the proposed MIMO-FD relaying system with SWIPT and that of MIMO half-duplex (HD) relaying systems with and without SWIPT. The validity of derived mathematical expressions is verified by Monte-Carlo simulations. Numerical results show that the TAS/MRC scheme gives better system performance than the TAS/SC scheme. Moreover, higher energy harvesting time is needed to maximize the throughput than to minimize the OP.

**Index Terms**—Multi-input multi-output, full-duplex, wireless power transfer, decode-and-forward, outage probability, symbol error probability, throughput.

## I. INTRODUCTION

NOWADAYS, full-duplex (FD) communication, has been used in many networks such as personal area networks and local area networks [1]. Furthermore, using relay can increase the quality-of-service, coverage, and reliability of wireless systems [2], [3]. Consequently, many studies have focused on analyzing the performance of full-duplex relaying (FDR) systems

in terms of the outage probability (OP), bit error rate (BER) and ergodic capacity [4]. It was shown that, although the residual self-interference (RSI) after interference suppression still exists and limits the performance of FD relay, FDR systems still have better capacity than the half-duplex relay (HDR) systems. A hybrid scheme that dynamically switches between FDR and HDR in a EH communication system was discussed in [5]. The authors concluded that FDR technique outperforms HDR and is an efficient relaying policy for harvest-use cooperative system. In [6], the authors considered a full-duplex multiple-antenna access point with half-duplex single antenna and spatially random users for simultaneous uplink/downlink transmissions. However, a key challenge in implementing a FDR transceiver is the presence of loopback interference. To overcome this limitation, in [7], [8], the authors proposed several SIC methods such as using directional antennas or employing the time-domain interference cancellation to isolate the Tx/Rx antennas.

On the other hand, the power supply for terminal devices in communication networks has attracted much attention from research institutions and scientists. Besides optimizing power allocation to reduce the power consumption in the fifth generation (5G) and sixth generation (6G) networks<sup>1</sup> such as in [10], another promising way to improve the operating duration of wireless communication devices is to convert external energy sources such as solar, wind, and RF signals to electric power to charge their batteries. Unfortunately, natural energy sources cannot be applied for small size mobile devices and in some cases cannot be used in healthcare monitoring networks, sensor networks, etc. On the other hand, compared with other kinds of sources, RF energy harvesting (EH), also known as simultaneous wireless information and power transfer (SWIPT), has some unique advantages such as full controllable and low cost [11], [12]. Thus, it is often used to prolong lifetime of passive powered devices [13]. In [14], an overview of recent advances in wireless power supply was provided, then several promising applications were presented to show the future trends. Besides, to efficiently schedule the harvested energy, an energy scheduling scheme in the EH-powered device-to-device (D2D) relay network was proposed as a case study. Another important consideration was the synchronization of switching time and decoding information in each time slot. It is useful for later research on designing antenna switching structure [15].

Currently, SWIPT has been used not only in the single-input single-output (SISO) systems but also in MIMO systems,

Manuscript received May 25, 2020; revised September 18, 2020 and November 17, 2020; accepted November 30, 2020. Date of publication December 8, 2020; date of current version January 22, 2021. The review of this article was coordinated by Dr. Maged Elkashlan. (*Corresponding author: Le The Dung.*)

Tran Manh Hoang and Ba Cao Nguyen are with the Telecommunications University, Khanh Hoa Province 650000, Vietnam, and also with the Advanced Wireless Communication Group, Le Quy Don Technical University, Ha Noi City 100000, Vietnam (e-mail: tranmanhhoang@tcu.edu.vn; nguyencbao@tcu.edu.vn).

Xuan Nam Tran is with the Faculty of Radio Electronics, and also with the Advanced Wireless Communication Group, Le Quy Don Technical University, Ha Noi City 100000, Vietnam (e-mail: namtx@mta.edu.vn).

Le The Dung is with the Division of Computational Physics, Institute for Computational Science, Ton Duc Thang University, Ho Chi Minh City 700000, Vietnam, and also with the Faculty of Electrical and Electronics Engineering, Ton Duc Thang University, Ho Chi Minh City 700000, Vietnam (e-mail: lethedung@tdtu.edu.vn).

Digital Object Identifier 10.1109/TVT.2020.3043015

<sup>1</sup>6G network will start entering market by 2026 [9].

because the multi-antennas are capable of converging energy by using beamforming techniques and they also provide spatial multiplexing gains. The MIMO system with SWIPT was investigated for the first time in [16]. Using the optimization problem, the authors found the maximum data rate and the maximum amount of harvested energy. In [17], the SWIPT MIMO technique was utilized in the multicell cooperative transmission environment, where multiple antennas at the users were separated into two sets, one for harvested energy and another for information decoding. However, this scheme is less applicable because the cost and complexity of the system remarkably increases with the number of antennas. The joint transceiver design algorithms for full duplex multi-pair MIMO with SWIPT were proposed in [18]. Specifically, the authors considered two optimization problems, i.e., the sum power minimization problem and the sum-rate maximization problem, to mitigate and exploit the complex interference. Unfortunately, they only applied SWIPT on one side of this two-way FD communication system. In [19], the authors demonstrated the performance gain by the optimal scheduling of EH for MIMO wireless powered communication networks comprising of a multi-antenna hybrid beamforming base station and multi-antenna users. It was shown that the number of required RF chains in hybrid beamforming decreases when using EH scheduling, and the performance gain in the EH time increases as network size increases and the number of RF chains decreases. However, the authors in [16]–[19] only considered the point-to-point MIMO system and did not compare the performance with other works. The negative impact of signal fading correlation in MIMO relaying system with perfect channel state information (CSI) on the performance of energy beamforming was studied in [20]. The authors of [21] analyzed the performance of MIMO-SWIPT relay network with imperfect CSI, especially they were able to derive the exact and approximate formula for the symbol error probability (SEP) of the EH networks. Unfortunately, the studies in [20] and [21] only analyzed MIMO half-duplex relaying (HDR) systems. In fact, HDR may not utilize the spectrum efficiently because two time slots are needed in one communication cycle. To overcome the limitation of MIMO-HDR systems, the optimal throughput of MIMO full-duplex system was proposed in [22]. However, the energy consumption at the relay is increased with its number of antennas.

Regarding to the research on transmit antenna selection (TAS)/maximal ratio combining (MRC) and TAS/selection combining (SC) schemes in the FD relay systems with multiple antennas at source destination, [23] and [24] evaluated the system performance with various values of the number of antennas at source and destination, including the special case of single antenna. Specifically, the authors of [23] investigated the secrecy outage performance of a dual-hop half-duplex (HD) MIMO relay system using the TAS/MRC scheme under the impact of outdated CSI and antenna configurations. They presented numerical results for different numbers of antennas at the source, relay, destination, and eavesdropper. It was shown that increasing the number of antennas at the source, relay and destination gives a growing positive effect on the secrecy outage performance while increasing the number of antennas at the eavesdropper

causes a negative impact. In [24], the outage performance of TAS and MRC in dual-hop full-duplex (FD) amplify-and-forward (AF) relay system over Rayleigh fading channels was studied. The authors plotted the system outage probability (OP) for different antenna configurations and claimed that as the number of antennas at the source increases, the floor level of the system OP decreases. Furthermore, for the same number of transmitting antennas, increasing the number of antennas at the destination does not decrease the floor level of the system OP, but increases diversity gain at the low SNR regime.

It is worth noticing that the performance of MIMO systems not only depends on the propagation environment but also on the gain of array configurations. Unfortunately, the complex time-varying wireless communication environment results in serve fluctuations in the amplitude and phase of the received signal, which then degrade the system performance significantly. When the error in estimating amplitude of channel happens, automatic gain control (AGC) can be used to properly scale the received signal. However, even in the absence of noise, when the phase component is estimated incorrectly, it will be very difficult to compensate the phase error of the received signals. More importantly, all previous works did not investigate the impact of outdated CSI on the system performance although the outdated CSI often happens in MIMO systems. In contrast, we study the effect of outdated CSI at the transmitter on the performance of a MIMO-FDR system with SWIPT at the relay.

The main contributions of our paper can be summarized as follows:

- We propose a MIMO-FDR system with SWIPT where multiple antennas are used at source and destination. This antenna configuration has more advantages than using multiple antennas at the relays [22] because it helps to share the operation complexity of relay to source and destination and provides better system performance in the high SNR region.
- We derive the closed-form expressions of the outage probability and the symbol error probability of the proposed MIMO-FDR system with SWIPT of TAS/SC and TAS/MRC schemes under the assumption of outdated CSI. The optimal time switching ratio  $\alpha$  that maximizes the throughput can be obtained by a closed-form expression while the optimal  $\alpha$  that minimizes the outage probability is determined through numerical results.
- The accurateness of all analysis results is validated by Monte-Carlo simulations. Numerical results show that TAS/MRC scheme provides better outage performance and throughput than TAS/SC scheme. Moreover, the value of time switching ratio that maximizes the throughput is larger than the value of time switching ratio that minimizes the outage probability.

The rest of this paper is organized as follows. Section II describes the MIMO-FDR system with SWIPT. Derivations of the outage probability and symbol error probability of the proposed protocol are presented in Section III. The optimization of system throughput is given in Section IV. Section V shows the numerical results obtained from both analyses and simulations. Finally, Section VI concludes the paper.

TABLE I  
THE MATHEMATICAL NOTATIONS USED IN THIS PAPER

Notation	Description
$F_U(u)$	Cumulative distribution function (CDF)
$f_U(u)$	Probability density function (PDF)
$\mathcal{CN}(\mu, \sigma^2)$	Complex Gaussian distribution with mean $\mu$ and variance $\sigma^2$
$\Gamma(\cdot)$	Gamma function
$\Gamma(\cdot, \cdot)$	Lower incomplete Gamma function
$\gamma_{th}$	Predefined outage threshold
$W(x)$	Lambert function [25]
$\mathcal{W}_{\ell, \mu}(z)$	Whittaker functions [25]
$\mathbb{E}\{\cdot\}$	Expectation operator
$\mathcal{K}_n(\cdot)$	The $n$ th order Bessel function of the second kind [25]
$I_0(\cdot)$	The modified zero order Bessel function of the first kind [25]
$\alpha$	Time switching ratio
$\eta$	Energy conversion efficiency
$\rho$	Channel correlation coefficient
$T$	Time block of a communication period
$\ \cdot\ _F$	Frobenius norm of a vector

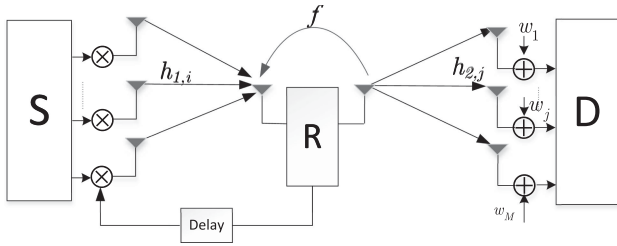


Fig. 1. Proposed MIMO-FDR system with SWIPT.

For the sake of clarity, frequently used mathematical notations together with their descriptions are summarized in Table I.

## II. SYSTEM MODEL

Fig. 1 illustrates a dual-hop communication FDR system of our consideration focusing, where source (S) and destination (D) have  $N$  and  $M$  antennas, respectively. In addition, we assume that the relay (R) process (reception/transmission) signals at two antennas independently.<sup>2</sup> The advantage of this proposed antenna configuration is to reduce the complexity and power consumption at R. Specifically, if multiple transmitting/receiving antennas are used at R, multiple RF chains are required for each antenna to perform the MRC/MRT scheme, leading to higher hardware complexity and power consumption. Meanwhile, from [7, Eqs. (9) and (16)], using a single transmitting/receiving antenna at the relay helps to reduce the residual interference power during full-duplex transmission significantly.

It is also assumed that the power supply from batteries is limited so that R has to rely on the harvested energy of signals transmitted from S [27]. Then, the energy harvested during the energy harvesting phase is stored in a super-capacitor,<sup>3</sup> and all harvested energy during EH phase is consumed by R during signal transmitting duration. In this system, the sizes of S, R, and D must be large enough to avoid mutual coupling between

antenna elements [29]. Specifically, a distance of greater or equal to half of wavelength between antenna elements is required.<sup>4</sup> Generally, direct S – D link not available when D is very far from S. However, as assumed in this paper, the direct S – D link may not exist even when the communication distance between S and D is short because the physical obstacles in dense urban environment such as buildings and mountains may block this direct S – D link.

In the proposed MIMO-FDR system with SWIPT, transmit antenna selection (TAS) scheme is utilized because it requires only a single RF chain, resulting in a considerable reduction in the size, cost, and complexity of transmitting antenna. Although the maximal ratio transmission (MRT) scheme has better performance, it requires multiple RF chains, making the complexity of the system are higher than the TAS scheme. The operation of this TAS scheme can be summarized as follows. First, S sends the pilot sequence one-by-one to R for the channel estimation. After that, R selects a transmit antenna associated with the  $i$ th best instantaneous SNR, and gives feedback on the index of the selected antenna to S. This feedback information can be presented by a binary vector with the number of bits  $b = \log_2 N$ .

Moreover, the distance between S and R cannot be very large due to the degradation of signal quality and the energy low conversion efficiency of SWIPT.<sup>5</sup> Modeling wireless channels by Rician or Nakagami- $m$  distributions may be more suitable, however, it results in an extremely high complexity when analyzing the performance of the proposed MIMO-FDR system with SWIPT. Alternatively, we analyze the system performance over quasi-static flat Rayleigh fading channels, which is the worst case. Therefore, if the proposed MIMO-FDR system with SWIPT fulfills all performance requirements over quasi-static flat Rayleigh-fading channel, it also works well over other kinds of wireless channels. For simplicity, we assume that all channel coefficients in a transmission block period  $T$  are constant but independent and identically distributed (i.i.d.) compared with those in other transmission block periods.

Let us denote  $h_{1,i} \sim \mathcal{CN}(0, \lambda_1)$  and  $h_{2,j} \sim \mathcal{CN}(0, \lambda_2)$  as the channel element vectors from S to the receiving antenna of R and from the transmitting antenna of R to D, respectively. For a slowly varying channel and the average fading power is supposed to remain constant over the time delay, i.e.,  $\mathbb{E}\{|\tilde{h}_{1,i}|^2\} = \mathbb{E}\{|h_{1,i}|^2\}$ , where  $\tilde{h}_{1,i}$  denotes the channel coefficient version of  $h_{1,i}$  in time-delayed. The average channel gains are  $\lambda_1 = \mathbb{E}\{|\hat{h}_{1,i}|^2\}$ ,  $\lambda_2 = \mathbb{E}\{|h_{RD}|^2\}$ . On the other hand,  $f \sim \mathcal{CN}(0, \lambda_3)$  is the channel coefficient of the transmitting antenna to the receiving antenna of R (a.k.a loopback channel) with  $\lambda_3 = \mathbb{E}\{|f|^2\}$  represents the strength of loopback channel. Since  $f$  is modeled by Rayleigh distribution.<sup>6</sup>  $|f|^2$  is

<sup>4</sup>This is the main limitation of designing practical MIMO systems.

<sup>5</sup>As mentioned in [30], SWIPT is applicable to (unmanned aerial vehicle) UAV-assisted communication systems where the UAV acts as a relay. It is because the altitude of the UAV is relatively short (ranging from 122 m to 300 m) and the line-of-sight (LoS) propagation mainly appears in UAV-ground channel.

<sup>6</sup>The loopback interference channel modeled by Rayleigh flat fading is a well-known model [7]. Notably, according to [6], the strong line-of-sight component of the loopback channel is removed during the interference canceling process at R. As a result, the loopback channel can be modeled as a Rayleigh fading channel.

<sup>2</sup>It is noted that a FD communication system equipped with a circulator can transmit and receive signals simultaneously with a single antenna [26].

<sup>3</sup>It is also called as harvest-use architecture [5], [28] which is different from harvest-store-use architecture.

exponentially distributed with mean  $\lambda_3$ . It is well-known that when channel coefficient follow Rayleigh distribution, channel gain will have exponential distribution. We should remind that  $|h_{SR}|^2 = \max_{i=1, \dots, N} |\tilde{h}_{1,i}|^2$  for TAS scheme. Denote  $\mathbf{h}_{RD} = [h_2^1, \dots, h_2^M]^*$  as the  $1 \times M$  channel vector from R to D, where  $(\cdot)^*$  refers to the transpose. Since selection combining (SC) scheme is applied at D, we have  $|h_{RD}|^2 = \max_{j=1, \dots, M} |h_{2,j}|^2$ . Additionally, when maximal ratio combining (MRC) scheme is applied, the weigh vector  $\mathbf{w}_R = \frac{\mathbf{h}_{RD}^\dagger}{\|\mathbf{h}_{RD}\|_F}$  is used to combine all antenna branches of D, where  $\dagger$  denotes the conjugate transpose operator and  $|h_{RD}|^2 = \sum_{j=1}^M |h_{2,j}|^2$ .

### A. The Impact of Outdated CSI on TAS Scheme

Due to the time-varying characteristics of S – R channel, its coherent time may be altered when the feedback delay is larger than the transmission block period  $T$ . Consequently, the feedback information of  $i$ th optimal antenna which is used to select antenna is outdated at S.<sup>7</sup> In [31], the authors considered that the second hop has weighting errors when combining the multiple received signals for MIMO with SWIPT system in HDR mode. However, the description of channel estimation errors in [31, Eq. (17)] may not suitable. In contrast, since R in our proposed MIMO-FDR system has only single antenna to transmit signals to multiple antennas of D, it does not require the feedback CSI from D. Thus, we only consider the outdated CSI sent from R to S to select the transmit antenna index. However, the outdated CSI may happen at D because it employs multiple antennas.

We denote  $\rho_{1,i}$  as the correlation coefficients between the past channel,  $h_{1,i}$ , and the current channel,  $\tilde{h}_{1,i}$ . For simplicity, we assume that the correlation coefficients  $\rho_{1,i}$  between  $\tilde{h}_{1,i}$  and  $h_{1,i}$  of all antennas at the S have the same values, i.e.,  $\rho_{1,i} = \rho$ , with  $i = 1, 2, \dots, N$  as the relative distance from the transmitting antennas of S to R can be considered to be equal. This assumption was also used in several previous works such as [32], [33].

Using Markov chain, the relationship of  $\tilde{h}_{1,i}$  and  $h_{1,i}$  can be modeled by the correlation coefficient  $\rho$  as [34]

$$\tilde{h}_{1,i} = \rho h_{1,i} + \sqrt{1 - \rho^2} e_{1,i}, \quad (1)$$

where  $0 \leq \rho \leq 1$ ;  $e_{1,i}$  is an error term due to temporal changes in the channel and is modeled by a circular symmetric complex Gaussian random variable. We can see that, the coefficient  $\rho$  depends only on the time delay and can be considered as the measurement of channel fluctuation rate. Moreover, as presented in [35], all random variables  $\tilde{h}_{1,i}, h_{1,i}, e_{1,i}$  are modeled by  $\mathcal{CN}(\mu, \sigma^2)$ . To reduce the complexity of mathematical equations, we denote  $X = |\tilde{h}_{1,i}|^2$  in the following analyses.

*Remark 1:* According to [36], [37], the PDF of the SNR of S – R link with TAS scheme in the case of outdated CSI is given by

$$f_X(x) = \sum_{i=1}^N \binom{N}{i} \frac{(-1)^{i-1} i}{\lambda_1 \Delta(\rho)} \exp\left(-\frac{ix}{\lambda_1 \Delta(\rho)}\right), \quad (2)$$

<sup>7</sup>In some cases, the phase and magnitude of the channel may be used normally even when the outdated feedback CSI happens. However, we do not consider this scenario in our paper.

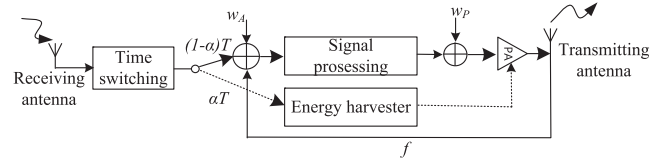


Fig. 2. Time switching based relaying protocol.

where  $\Delta(\rho) = 1 + (i - 1)(1 - \rho^2)$ .

*Proof:* Please refer to [36] and [37]. ■

From (2), we have the CDF of  $X$  as

$$F_X(x) = \sum_{i=1}^N \binom{N}{i} (-1)^{i-1} \left[ 1 - \exp\left(-\frac{ix}{\lambda_1 \Delta(\rho)}\right) \right]. \quad (3)$$

Based on the property of CDF, i.e.,  $F_X(\infty) = 1$ , then when  $x \rightarrow \infty$  in (3),  $\sum_{i=1}^N \binom{N}{i} (-1)^{i-1} = 1$ . Then, we can rewrite (3) as

$$F_X(x) = 1 - \sum_{i=1}^N \binom{N}{i} (-1)^{i-1} \exp\left(-\frac{ix}{\lambda_1 \Delta(\rho)}\right). \quad (4)$$

The PDF in (2) and CDF in (4) are the probability functions which model the statistics of the instantaneous SINR at R with outdated CSI. From these equations, we can see that when the outdated CSI happens, the variance of fading channel amplitude increases, making the system performance decrease.

We should note that D linearly combines the received signals from its  $M$  receiving antennas. These signals are transmitted by an antenna of R. This technique is also called as receive beamforming. Moreover, R does not request feedback CSI from D. For simplicity, we assume that the CSI of R – D link is perfect.

### B. TSR Protocol

For current technologies, the operating sensitivity of the information receiver is different from that of the energy receiver (i.e.,  $-10$  dBm for energy harvesters versus  $-60$  dBm for information receivers). To overcome this limitation, the authors of [27] proposed two practical receiver architectures, i.e., power splitting relaying (PSR) and time switching relaying (TSR), which allow the receiver to decode information and harvest energy. In [38], the authors showed that a multi-user FD system using the TS scheme has a higher throughput than that system using the PS scheme. Thus, we only consider the TSR scheme at R in this paper.

The communicating process from source to destination in a RF energy harvesting full duplex communication system is described as follows. Let  $T$  denote the time block of an entire communication period in which the information is transmitted from S to D. For every  $T$  period, the first amount of time  $\alpha T$  is used for energy harvesting at R while the remaining amount of time  $(1 - \alpha)T$  is used for information transmission and reception, where  $\alpha$ ,  $0 \leq \alpha < 1$ , denotes the percentage of the block time  $T$  for energy harvesting as illustrated in Fig. 2. It should be noted that the case  $\alpha = 1$  is not considered in this paper because when the energy harvesting time duration takes the whole communication period  $T$ , the relay does not process

any signals. Thus, the basic role in signal forwarding of the relay is eliminated [15].

As presented in [22], [39], the amount of harvested energy during  $\alpha T$  with linear EH model and using the TAS technique is calculated as

$$E_h = P_S \eta \alpha T \max_{i=1, \dots, N} |\tilde{h}_{1,i}|^2, \quad (5)$$

where  $0 < \eta \leq 1$  is the energy conversion efficiency which depends on the quality of energy conversion circuitry [15].

From (5), the transmission power of R is expressed as<sup>8</sup>

$$P_R = \frac{E_h}{1 - \alpha} = \phi P_S \max_{i=1, \dots, N} |\tilde{h}_{1,i}|^2, \quad (6)$$

where  $\phi = \alpha \eta / (1 - \alpha)$ .

We can see that the transmission power of R depends on the amount of energy harvested during EH phase. On the other hand, the amount of harvested energy is determined by the wavelength, the power of RF signals, as well as the distance between harvesting node and RF energy source.

### III. PERFORMANCE ANALYSIS

In this section, we will derive the mathematical expressions of the outage probabilities (OPs) for both TAS/SC and TAS/MRC schemes. Then, based on these OP expressions, we derive the closed-form expressions of SEPs. The purpose of analyzing the OP and SEP of the proposed MIMO-FDR system with SWIPT using both TAS/SC and TAS/MRC schemes is to clearly show the differences in the system performance corresponding to these two schemes so that network designers can rely on these results to make useful decisions. A similar comparison was also presented in [40].

After the first time slot for energy harvesting, the signal processing is performed in the second time slot. We assume that the delay caused by the signal processing at R is equal to one period to guarantee that current transmitted symbol is uncorrelated with the received symbol [6], [7]. In other word, the signal transmitted at R is the received signal from S in the previous period. Therefore, the received signal at R are presented as

$$y_R(k) = h_{SR} \sqrt{P_S} x(k) + f \sqrt{P_R} \tilde{x}(k - \tau) + n_R(k), \quad (7)$$

where  $P_S$  and  $P_R$  denote for transmission power of S and R, respectively;  $x(k)$  and  $\tilde{x}(k - \tau)$  are the signals at S and R, respectively;  $\tau$ ,  $\tau > 0$ , is an integer processing delay (in the number of time slots) due to the signal processing at the FD relay;  $n_R(k)$  is the additive white Gaussian noise (AWGN) at R

which follows normal distribution with zero-mean and variance of  $\sigma_R^2$ , i.e.,  $n_R(k) \sim \mathcal{CN}(0, \sigma_R^2)$ .

It is worth noticing that, in the case that the channel from the transmitting antenna to the receiving antenna of R has perfect CSI and the hardware of R is ideal, there is no RSI after SIC. Thus, the term  $f \sqrt{P_R} \tilde{x}(k - \tau)$  does not appear in (7). In other words, by giving  $f \sqrt{P_R} \tilde{x}(k - \tau)$  in (7), we imply that  $f$  is imperfect. Furthermore, as presented in [41],  $n_R(k)$  is much smaller than  $\sqrt{P_R} f \tilde{x}(k - \tau)$ , i.e., the thermal noise at relay is much smaller than SI, thus we can ignore this thermal noise. On the other hand, R knows the transmitted signal  $\tilde{x}(k - \tau)$  and combines it with the estimated SI channel  $f$  to subtract the SI from the received signals by using analog and digital methods [7].<sup>9</sup>

After R decodes successfully the signals and forwards to D, the received signal at D is

$$y_D(k) = \sqrt{P_R} \mathbf{h}_{RD} \tilde{x}(k) + \mathbf{n}_D(k), \quad (8)$$

where  $\mathbf{n}_D$  is the AWGN matrix with i.i.d. elements at D follow the normal distribution with zero-mean and variance  $\sigma_D^2$ , which is mathematically modeled as  $\mathbf{n}_D \sim \mathcal{CN}(0, \sigma_D^2 \mathbf{I}_M)$  with  $\mathbf{I}_M \in \mathbb{C}^{M \times 1}$  is the identity matrix. From the received signal (7) and (8), we can present the SINRs of S-R and R-D links as

$$\gamma_{SR} = \frac{P_S |h_{SR}|^2}{P_R |f|^2 + \sigma_R^2}. \quad (9)$$

$$\gamma_{RD} = \frac{P_R \|\mathbf{h}_{RD}\|^2}{\sigma_D^2}. \quad (10)$$

According to DF protocol, the end-to-end SINR is given by

$$\gamma_{e2e} = \min(\gamma_{SR}, \gamma_{RD}). \quad (11)$$

The OP is defined as the probability that the instantaneous error probability exceeds a specified value. In other words, it is the probability that the output SNR falls below a certain threshold. Therefore, the OP can be computed as

$$\begin{aligned} \text{OP} &= \Pr [(1 - \alpha) \log_2 (1 + \gamma_{e2e}) \leq \mathcal{R}] \\ &= \Pr (\min(\gamma_{SR}, \gamma_{RD}) \leq \gamma_{th}), \end{aligned} \quad (12)$$

where  $\gamma_{th} = 2^{\frac{\mathcal{R}}{1-\alpha}} - 1$  is a predefined outage threshold served as the protected values of SNR to ensure the quality of service of the system,  $\mathcal{R}$  is a predefined end-to-end spectral efficiency, i.e., the total bits per channel usage.

#### A. TAS/SC Scheme

In this subsection, we investigate the OP and SEP of the proposed MIMO-FDR system with SWIPT using TAS/SC scheme.<sup>10</sup>

<sup>9</sup>SIC methods includes natural isolation, time-domain cancellation, and spatial suppression. Especially, SIC methods in FD techniques, including passive suppression, active analog cancellation, and active digital cancellation, can suppress the self-interference up to 110 dB [26].

<sup>10</sup>When TAS is used with SC, the scheme is commonly denoted as TAS/SC, so on TAS/MRC.

<sup>8</sup>In practice, the output power of EH circuit may be proportional to the harvested input power up to a certain power threshold  $P_{th}$ . As the input power exceeds  $P_{th}$ , the output power remains unchanged. This nonlinear EH model reflects the joint effect of of the light sensitivity limit and the current leakage of EH circuit. Due to this nonlinear characteristic, the transmission power of R in the case of nonlinear EH model can be obtained by extending (6), i.e.,

$$P_R = \begin{cases} \frac{2\alpha\eta}{1-\alpha} P_S \max_{i=1, \dots, N_S} |\tilde{h}_{1,i}|^2, & P_S \max_{n=1, \dots, N} |\tilde{h}_{1,i}|^2 \leq P_{th} \\ \frac{2\alpha\eta}{1-\alpha} P_{th}, & P_S \max_{i=1, \dots, N_S} |\tilde{h}_{1,i}|^2 > P_{th}. \end{cases}$$

From (6), (9), and (10), the SINRs of the best S–R link and R–D link are given in (13) and (14), respectively.

$$\gamma_{\text{SR}} = \frac{P_{\text{S}} \max_{i=1,\dots,N} |\tilde{h}_{1,i}|^2}{\phi P_{\text{S}} \max_{i=1,\dots,N} |\tilde{h}_{1,i}|^2 |f|^2 + \sigma_{\text{R}}^2}, \quad (13)$$

$$\gamma_{\text{RD}} = \frac{\phi P_{\text{S}}}{\sigma_{\text{D}}^2} \max_{i=1,\dots,N} |\tilde{h}_{1,i}|^2 \max_{j=1,\dots,M} |h_{2,j}|^2. \quad (14)$$

Dividing both numerator and denominator of (13) by  $\sigma_{\text{R}}^2$ , we have

$$\gamma_{\text{SR}} = \frac{\frac{P_{\text{S}}}{\sigma_{\text{R}}^2} \max_{i=1,\dots,N} |\tilde{h}_{1,i}|^2}{\phi \frac{P_{\text{S}}}{\sigma_{\text{R}}^2} \max_{i=1,\dots,N} |\tilde{h}_{1,i}|^2 |f|^2 + 1}. \quad (15)$$

Generally, the transmission power of S is much higher than thermal noise. Thus,  $\phi \frac{P_{\text{S}}}{\sigma_{\text{R}}^2} \max_{i=1,\dots,N} |\tilde{h}_{1,i}|^2 |f|^2 \gg 1$ . Then,  $\gamma_{\text{SR}}$  can be approximated as<sup>11</sup>

$$\gamma_{\text{SR}} \approx \frac{1}{\phi |f|^2}. \quad (16)$$

*Proposition 1:* The OP of the proposed MIMO-FDR system with SWIPT using TAS/SC scheme in the condition of outdated CSI is given by

$$\begin{aligned} \text{OP}_{\text{SC}} &= 1 - \sum_{i=1}^N (-1)^{i+j-2} \sum_{j=1}^M \binom{M}{j} \binom{N}{i} \left[ 1 - e^{-\frac{1}{\phi \lambda_3 \gamma_{\text{th}}}} \right] \\ &\times \sqrt{\frac{4ij\gamma_{\text{th}}\sigma_{\text{D}}^2}{\phi P_{\text{S}} \lambda_1 \Delta(\rho) \lambda_2}} \mathcal{K}_1 \left( \sqrt{\frac{4ij\gamma_{\text{th}}\sigma_{\text{D}}^2}{\phi P_{\text{S}} \lambda_1 \Delta(\rho) \lambda_2}} \right), \quad (17) \end{aligned}$$

where  $\Delta(\rho) = 1 + (i-1)(1-\rho^2)$  indicates the severity of the time delay of CSI are feedback from R to S,  $\mathcal{K}_n(\cdot)$  is the  $n$ th order Bessel function of the second kind [25].

*Proof:* When using SC technique, the SNR obtained at destination is the highest SNR among antenna branches for decoding. Let  $Y = \max_{j=1,\dots,M} |h_{2,j}|^2$  be the product of independent random variables. Using [42, Eq. (7–14)], the PDF of  $Y$  can be given by

$$f_Y(y) = \sum_{j=1}^M (-1)^{j-1} \binom{M}{j} \frac{j}{\lambda_2} \exp\left(-\frac{ jy}{\lambda_2}\right). \quad (18)$$

From (15) and (14), the end-to-end SINR,  $\gamma_{\text{e2e}}$ , can be rewritten as

$$\gamma_{\text{e2e}} = \min\left(\frac{1}{\phi |f|^2}, \frac{\phi P_{\text{S}} XY}{\sigma_{\text{D}}^2}\right). \quad (19)$$

Let  $\mathcal{Z} = XY$ , we can rewrite the joint CDF of  $X$  and  $Y$  as the CDF of  $\mathcal{Z}$  as

$$F_{\mathcal{Z}}(z) = \Pr(XY < z) = \int_0^\infty F_X\left(\frac{z}{y}\right) f_Y(y) dy. \quad (20)$$

<sup>11</sup>For the sake of simplicity, the thermal noise at R is omitted in mathematical analyses. However, it is still taken into consideration in simulations.

When the channel coefficients follow Rayleigh distributions, the channel gains follow exponential distributions. Substituting (3) and (18) into (20), we obtain

$$F_{\mathcal{Z}}(z) = 1 - \Psi(\Sigma, N, M) \frac{j}{\lambda_2} \int_0^\infty \exp\left(-\frac{iz}{y\lambda_1\Delta(\rho)} - \frac{ jy}{\lambda_2}\right) dy. \quad (21)$$

To get the closed-form of (21), we use [25, Eq. (3.324.1)], then, we have the CDF of  $\mathcal{Z}$  as

$$F_{\mathcal{Z}}(z) = 1 - \Psi(\Sigma, N, M) \sqrt{\frac{4ijz}{\lambda_1\Delta(\rho)\lambda_2}} \mathcal{K}_1\left(\sqrt{\frac{4ijz}{\lambda_1\Delta(\rho)\lambda_2}}\right), \quad (22)$$

where

$$\Psi(\Sigma, N, M) = \sum_{i=1}^N \sum_{j=1}^M (-1)^{i+j-2} \binom{N}{i} \binom{M}{j}.$$

From the OP derived in (12) and let  $W = |f|^2$ , we can rewrite the expression of OP as

$$\begin{aligned} \text{OP} &= \Pr\left[\min\left(\frac{1}{\phi W}, \frac{\phi P_{\text{S}} \mathcal{Z}}{\sigma_{\text{D}}^2}\right) < \gamma_{\text{th}}\right] \\ &= 1 - \Pr\left[\frac{1}{\phi W} > \gamma_{\text{th}}, \frac{\phi P_{\text{S}} \mathcal{Z}}{\sigma_{\text{D}}^2} > \gamma_{\text{th}}\right], \quad (23) \end{aligned}$$

where  $\gamma_{\text{th}} = 2^{\mathcal{R}/(1-\alpha)} - 1$  denotes the SNR threshold at D at which the information from S can be decoded successfully at the target rate  $\mathcal{R}$ .

We see that  $W$  and  $\mathcal{Z}$  in (23) are independent random variables. Thus, we can rewrite (23) becoming as

$$\begin{aligned} \text{OP} &= 1 - \Pr\left(W < \frac{1}{\gamma_{\text{th}}\phi}\right) \Pr\left(\mathcal{Z} > \frac{\gamma_{\text{th}}\sigma_{\text{D}}^2}{\phi P_{\text{S}}}\right) \\ &= 1 - \left[1 - \exp\left(-\frac{1}{\gamma_{\text{th}}\phi\lambda_3}\right)\right] \left[1 - F_{\mathcal{Z}}\left(\frac{\gamma_{\text{th}}\sigma_{\text{D}}^2}{\phi P_{\text{S}}}\right)\right]. \quad (24) \end{aligned}$$

Finally, plugging (22) into (24), we have the OP expression as in (17). The proof of Proposition 1 is completed. ■

Another performance criterion which is undoubtedly the most difficult one to analyze is the average SEP. Hence, this criterion has not been investigated in the previous works on SWIPT systems. We will derive the expressions of SEP for TAS/SC scheme in the following Theorem 1.

*Theorem 1:* The SEP of the proposed MIMO-FDR system with SWIPT using TAS/SC scheme in the condition of outdated CSI is given by

$$\text{SEP}_{\text{TAS/SC}} = \frac{a}{2} - [\mathcal{I}_1 - \mathcal{I}_2], \quad (25)$$

$\mathcal{I}_1$  is given in (26), shown at the bottom of the next page, and

$$\begin{aligned} \mathcal{I}_2 &= \sum_{i=1}^N \sum_{j=1}^M (-1)^{i+j-2} \binom{N}{i} \binom{M}{j} a \sqrt{\frac{b}{\pi}} \\ &\times \left(\frac{1}{\phi\lambda_3 b}\right)^{\frac{1}{4}} \mathcal{K}_{\frac{1}{2}}\left(2\sqrt{\frac{b}{\phi\lambda_3}}\right), \quad (27) \end{aligned}$$

where  $a$  and  $b$  are the constants whose values depend on modulation types, e.g., ( $a = 1, b = 1$ ) for binary phase-shift keying (BPSK) modulation and ( $a = 2, b = \sin^2(\frac{\pi}{M})$ ) for  $M$ -PSK modulation. In this paper, we only consider BPSK modulation.

*Proof:* When detecting  $M$ -PSK signals, SEP is described as [43], i.e.,  $\text{SEP} = aQ(\sqrt{2b\gamma_{e2e}})$ .

After having the CDF of SNR, the average SEP can be calculated as

$$\text{SEP} = a \int_0^\infty Q\left(\sqrt{2b\gamma_{e2e}}\right) f_{\gamma_{e2e}}(\gamma) d\gamma, \quad (28)$$

where  $Q(x) = (1/\sqrt{2\pi}) \int_x^\infty e^{-t^2/2} dt$  is the Gaussian Q-function. Then, the average SEP of the system is

$$\text{SEP} = \frac{a\sqrt{b}}{2\sqrt{\pi}} \int_0^\infty \frac{e^{-b\gamma}}{\sqrt{\gamma}} F_{\gamma_{e2e}}(\gamma) d\gamma. \quad (29)$$

We should remind that the OP is the CDF of the instantaneously SNR, i.e.,  $\text{OP} = \int_0^{\gamma_{\text{th}}} f_X(x) dx = F_X(x)$  [44, Eq. (1.4)]. From the expression of OP presented in (17), after some manipulations, we obtain  $\text{SEP}_{\text{TAS/SC}}$  as in (25). Please refer to Appendix A for detailed derivations. ■

*Remark 2:* It is noted that, when the TAS/SC scheme is used, the impacts of the numbers of antennas at S and D on the system performance are similar. Furthermore, the OP and SEP are greatly influenced by the arguments of the first-order modified Bessel function of the second kind.

## B. TAS/MRC Scheme

*Proposition 2:* The OP of the proposed MIMO-FDR system with SWIPT using TAS/MRC scheme under outdated CSI is given by

$$\begin{aligned} \text{OP}_{\text{MRC}} &= 1 - \sum_{i=1}^N (-1)^{i-1} \binom{N}{i} \left[ 1 - e^{-\frac{1}{\phi\lambda_3\gamma_{\text{th}}}} \right] \\ &\quad \times \frac{2}{\Gamma(M)\lambda_2^M} \left( \frac{i\gamma_{\text{th}}\sigma_D^2\lambda_2}{\phi P_S\lambda_1\Delta(\rho)} \right)^{\frac{M}{2}} \\ &\quad \times \mathcal{K}_M \left( 2\sqrt{\frac{i\gamma_{\text{th}}\sigma_D^2}{\lambda_1\Delta(\rho)\lambda_2\phi P_S}} \right), \quad (30) \end{aligned}$$

where  $\Gamma(M)$  is the Gamma function.

*Proof:* When MRC technique is used at D, the  $\gamma_{\text{RD}}$  is

$$\gamma_{\text{RD}} = \frac{\phi P_S}{\sigma_D^2} \max_{i=1, \dots, N} |\tilde{h}_{1,i}|^2 \sum_{j=1}^M |h_{2,j}|^2. \quad (31)$$

We let  $Y = \sum_{j=1}^M |h_{2,j}|^2$ . Thus, the CDF and PDF of  $Y$  are respectively given by [45]

$$F_Y(y) = 1 - e^{-\frac{y}{\lambda_2}} \sum_{j=0}^{M-1} \frac{1}{j!} \left( \frac{y}{\lambda_2} \right)^j. \quad (32)$$

$$f_Y(y) = \frac{y^{M-1} e^{-\frac{y}{\lambda_2}}}{\Gamma(M)\lambda_2^M}. \quad (33)$$

Note that the PDF of  $X$  given in (2). Similar to (20), the CDF of  $\mathcal{Z}$  is calculated as

$$F_{\mathcal{Z}}(z) = 1 - \mathcal{A}_{\mathcal{X}}(\Sigma, N, M) \int_0^\infty y^{M-1} \exp\left(-\frac{iz}{y\lambda_1\Delta(\rho)} - \frac{y}{\lambda_2}\right) dy, \quad (34)$$

where  $\mathcal{A}_{\mathcal{X}}(\Sigma, N, M) = \sum_{i=1}^N (-1)^{i-1} \binom{N}{i} \frac{1}{\Gamma(M)\lambda_2^M}$ . Using [25, Eq. (3.471.9)], then (34) can be rewritten as

$$\begin{aligned} F_{\mathcal{Z}}(z) &= 1 - 2\mathcal{A}_{\mathcal{X}}(\Sigma, N, M) \left( \frac{iz\lambda_2}{\lambda_1\Delta(\rho)} \right)^{\frac{M}{2}} \mathcal{K}_M \left( 2\sqrt{\frac{iz}{\lambda_1\Delta(\rho)\lambda_2}} \right). \quad (35) \end{aligned}$$

Finally, from the expression of OP in (23), we substitute (35) into (24) to obtain the expression of OP as in (30). ■

Based on the  $\text{OP}_{\text{MRC}}$  in (30), we can derive the SEP of TAS/MRC scheme in the following Theorem 2.

*Theorem 2:* The SEP of the proposed MIMO-FDR system with SWIPT using TAS/MRC scheme under outdated CSI is given by

$$\text{SEP}_{\text{TAS/MRC}} = \frac{a}{2} - [\mathcal{I}_3 - \mathcal{I}_4], \quad (36)$$

where  $\mathcal{I}_3$  is given in (37), shown at the bottom of this page, and

$$\mathcal{I}_4 = \sum_{i=1}^N (-1)^{i-1} \binom{N}{i} a \sqrt{\frac{b}{\pi}} \left( \frac{1}{2} \right)^{\frac{M}{2}} \left( \frac{1}{\phi\lambda_3 b} \right)^{\frac{1}{4}} \mathcal{K}_{\frac{1}{2}} \left( 2\sqrt{\frac{b}{\phi\lambda_3}} \right), \quad (38)$$

with  $\mathcal{W}_{\ell, \mu}(z)$  is the Whittaker function [25].

$$\mathcal{I}_1 = \sum_{i=1}^N \sum_{j=1}^M \binom{N}{i} \binom{M}{j} \exp\left(\frac{ij\sigma_D^2}{2\phi P_S\lambda_1\Delta(\rho)\lambda_2}\right) \frac{aij\sigma_D^2(-1)^{i+j-2}}{2\phi P_S\lambda_1\Delta(\rho)\lambda_2} \left[ \mathcal{K}_1\left(\frac{ij\sigma_D^2}{2\phi P_S\lambda_1\Delta(\rho)\lambda_2}\right) - \mathcal{K}_0\left(\frac{ij\sigma_D^2}{2\phi P_S\lambda_1\Delta(\rho)\lambda_2}\right) \right] \quad (26)$$

$$\begin{aligned} \mathcal{I}_3 &= \sum_{i=1}^N (-1)^{i-1} \binom{N}{i} \frac{a\sqrt{b}}{\sqrt{\pi}} \frac{1}{\Gamma(M)\lambda_2^M} \left( \frac{i\sigma_D^2\lambda_2}{\phi P_S\lambda_1\Delta(\rho)} \right)^{\frac{M}{2}} \frac{\Gamma(M + \frac{1}{2})\Gamma(\frac{1}{2})}{\sqrt{\frac{i\sigma_D^2}{\phi P_S\lambda_1\Delta(\rho)\lambda_2}}} \\ &\quad \times \exp\left(\frac{i\sigma_D^2}{2b\phi P_S\lambda_1\Delta(\rho)\lambda_2}\right) b^{-\frac{M}{2}} \mathcal{W}_{-\frac{M}{2}, \frac{M}{2}} \left( \frac{i\sigma_D^2}{b\phi P_S\lambda_1\Delta(\rho)\lambda_2} \right) \quad (37) \end{aligned}$$

*Proof:* We begin with the  $OP_{MRC}$  given in (30) and reuse (29) to proof Theorem 2 similarly as in Theorem 1. Please refer to Appendix B. ■

*Remark 3:* It is noted that, when the TAS/MRC scheme is used, the number of antennas at D (i.e.,  $M$ ) has a dominating effect on the system performance. Specifically,  $M$  is the variable of Gamma function and the  $M$  order of Bessel function in (30), and the  $M/2$  order of Whittaker function in (37). This is the main difference between the TAS/SC and TAS/MRC schemes.

#### IV. OPTIMIZATION OF SYSTEM THROUGHPUT

The throughput, is defined as the ratio of the average number of packets successfully transmitted in any given time interval to the number of attempted transmissions in that interval. It is generally calculated from the OP of the system at a fixed transmission rate of  $\mathcal{R}$  bits/sec/Hz [46]. Let  $\mathcal{R}$  be a fixed transmission rate satisfying  $\mathcal{R} = \log_2(1 + \gamma_{th})$ , where  $\gamma_{th}$  is the SNR threshold for correct data detection. From [27, Eq. (14)] and the operation of TS protocol, we can derive the throughput expression of FDR system as

$$R_{ID}(\alpha) = \mathcal{R}(1 - \alpha)(1 - OP). \quad (39)$$

The aim of this section is to find the TS ratio  $\alpha$  that maximizes the throughput. Unfortunately, from (39), it is very difficult to obtain the closed-form expression of optimal throughput with respect to  $\alpha$ . Another way to calculate the system throughput is to use the instantaneous capacity with acceptable delay, which is the upper bound of the data rate that system can achieve with arbitrary coding length. From (11), we can rewrite the instantaneous capacity of the proposed MIMO-FDR system with SWIPT as

$$R_{ID}(\alpha) = (1 - \alpha) \times \log_2 \left( 1 + \min \left\{ \frac{\eta\alpha|f|^2}{1 - \alpha}, \frac{\eta\alpha P_S |h_{SR}|^2 ||\mathbf{h}_{RD}|^2}{(1 - \alpha)\sigma_D^2} \right\} \right). \quad (40)$$

We can see that (40) shows the trade-off between the time switching ratio  $\alpha$  and the throughput. Specifically, if  $\alpha$  is high, the harvested energy will be increased. Then, the SNR of the second hop is improved. However, the drawback is the time duration for information transmission of the first hop is shortened. Hence, it is necessary to optimize the value of  $\alpha$  to balance the throughput and the amount of harvested energy.

The optimal value of  $\alpha$  can be obtained by solving the optimization problem

$$\begin{aligned} \alpha_{opt} &= \arg \max_{\alpha} R_{ID}(\alpha), \\ \text{subject to } & 0 \leq \alpha \leq 1 \end{aligned} \quad (41)$$

whose solution is presented in the following Theorem 3.

*Theorem 3:* The optimal value of  $\alpha$ ,  $\alpha_{opt}$ , which maximizes the upper bound throughput of the proposed MIMO-FDR system

with SWIPT is given by

$$\alpha_{opt} = \begin{cases} \frac{e^{W\left(\frac{c_0-1}{e}\right)+1}-1}{c_0-1+e^{W\left(\frac{c_0-1}{e}\right)+1}}, & (42a) \\ \text{if } e^{W\left(\frac{c_0-1}{e}\right)+1} < \frac{c_1(\sqrt{c_0c_1}-1)}{2\sqrt{c_0c_1+1}}; & (42b) \\ \frac{\sqrt{c_0c_1}-1}{1-c_0c_1}, & \text{otherwise,} \end{cases}$$

where  $W(x)$  is the Lambert  $W$  function [47],  $x$  is the solution to the equation  $W(x) \exp(W(x)) = x$ ,  $b_0 = |h_{SR}|^2 ||\mathbf{h}_{RD}|^2$ ,  $c_0 = \frac{\eta P_S |f|^2}{\sigma_D^2}$ , and  $c_1 = \eta b_0$ .

This  $\alpha_{opt}$  can be used to minimize the OP and SEP, and maximize the throughput.

*Proof:* We consider two following cases of (40).

The first case is when  $0 < \alpha < \frac{\sqrt{c_0c_1}-1}{1-c_0c_1}$ , we have

$$R_{ID}(\alpha) = \frac{(1 - \alpha)}{\ln 2} \ln \left( 1 + \frac{\eta\alpha P_S |f|^2}{(1 - \alpha)\sigma_D^2} \right). \quad (43)$$

Taking the partial derivation of (43) with respect to  $\alpha$ , and letting this derivation be equal to zero, we have

$$c_0 + \frac{c_0\alpha}{1 - \alpha} = \left( 1 + \frac{c_0\alpha}{1 - \alpha} \right) \ln \left( 1 + \frac{c_0\alpha}{1 - \alpha} \right), \quad (44)$$

After some manipulations, we obtain

$$\frac{c_0 - 1}{e} = \ln \left( \frac{u}{e} \right) e^{\ln \left( \frac{u}{e} \right)}, \quad u = \frac{c_0\alpha}{1 - \alpha} + 1. \quad (45)$$

Using [47, Eq. (1.5)] and after some manipulations, we have the optimal value  $\alpha^*$  as in (42a).

We now investigate the case that  $\alpha$  ranges over  $\frac{\sqrt{c_0c_1}-1}{1-c_0c_1} \leq \alpha < 1$ . Then, we can rewrite (43) as

$$R_{ID}(\alpha) = \frac{(1 - \alpha)}{\ln 2} \ln \left( 1 + \frac{1 - \alpha}{\eta\alpha b_0} \right). \quad (46)$$

Taking the partial derivation of  $R_{ID}(\alpha)$  in (46) with respect to  $\alpha$ , we have

$$\frac{\partial R_{ID}(\alpha)}{\partial \alpha} = \frac{-\frac{(1-\alpha)^2}{\eta|f|^2\alpha^2} - \frac{1-\alpha}{\eta|f|^2\alpha}}{\frac{1-\alpha}{\eta b_0\alpha} + 1} - \ln \left( 1 + \frac{1 - \alpha}{\eta b_0\alpha} \right). \quad (47)$$

We can easily see that (47) is always less than zero, thus,  $R_{ID}(\alpha)$  is a decreasing function. Obviously,  $\alpha = \frac{\sqrt{c_0c_1}-1}{1-c_0c_1}$  is the value at which the system throughput is maximal. ■

#### V. NUMERICAL RESULTS AND DISCUSSIONS

In this section, we study the effects of the number of antennas at S and D on the OP, SEP, and throughput of the proposed MIMO-FDR system with SWIPT using TAS/SC and TAS/MRC schemes. When not explicitly mentioned, the parameter settings are as follows. The data rate threshold  $\mathcal{R}_{th} = 1$  bit/s/Hz. The energy conversion efficiency  $\eta = 0.85$ . The time switching ratio  $\alpha = 0.3$ . In this system, we only consider small-scale Rayleigh fading and assume that the terminals are stationary. Thus, the path losses from the source to relay and from relay to destination are characterized as average gains  $\lambda_{1,i} = \mathbb{E}\{|\hat{h}_{1,i}|^2\} = 1$  and  $\lambda_{2,j} = \mathbb{E}\{|\hat{h}_{RD}|^2\} = 1$ , ( $i = 1, \dots, N; j = 1, \dots, M$ ), respectively. The distances are normalized, i.e.,  $d_{SR} = d_{RD} = 1$ , and the average SNR is defined as the ratio of the transmission

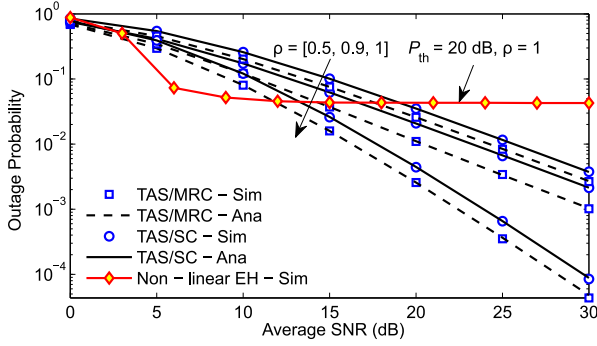


Fig. 3. Outage probability of TAS/SC scheme versus the average SNR for different correlation coefficients  $\rho$ .  $N = M = 2$ .

power to the variance of AWGN, i.e.,  $\text{SNR} = P_S/\sigma^2$ . Without loss of generality, we let  $\sigma_R^2 = \sigma_D^2 = \sigma^2 = 1$ . According to the standards of LTE and IEEE 802.11a/g [48], [49], the average channel gain of the SI channel is  $\lambda_3 = 0.05$ . In some evaluating scenarios, we set the number of antennas at source and destination  $[N, M] = [1, 1]$  to compare the performance of our proposed MIMO-FDR system with that of the conventional single-antenna FDR system.

Fig. 3 plots the OPs of TAS/SC and TAS/MRC schemes versus the average SNR in dB for different channel correlation coefficients  $\rho$  and  $[N, M] = [2, 2]$ . As shown in Fig. 3, increasing  $\rho$  lowers the OP because of the decreased delay of feedback information from R to S. However, the improvement is only significant as  $\rho$  approaches 1, which is the case of perfect CSI. Hence, the channel correlation coefficient has a strong effect on the outage performance. We can also see that although a part of signal period  $T$  is used for EH, the diversity order remains approximately being equal to two when the CSI is perfect. Therefore, if the time switching ratio  $\alpha$  is properly chosen, the achievable quality of the proposed MIMO-FDR system with SWIPT can be similar to that of conventional MIMO system, diversity orders are in the range of  $\min(N, M)$  approximately. We provide the OP of the TAS/SC scheme in the case of non-linear EH to compare with that in the case of linear EH. From Fig. 3, the OP of the TAS/SC scheme with linear EH continuously decreases as the average SNR gets higher while the OP of the TAS/SC scheme with non-linear EH reaches the saturated value of 0.04 as the average SNR exceeds 12 dB. Even with  $P_{\text{th}} = 20$  dB, which is a slightly high threshold, this OP is still high.

Fig. 4 demonstrates the OPs of TAS/SC and TAS/MRC schemes versus the average SNR in dB for different  $[N, M]$  pairs. We consider three  $[N, M]$  pairs, i.e.,  $[N, M] = [1, 1]$ ,  $[N, M] = [2, 2]$ , and  $[N, M] = [3, 3]$ . The channel correlation coefficient  $\rho$  is fixed at 0.8. As observed from Fig. 4, when  $N$  and  $M$  increase, the outage performance is improved. Moreover, we can see from Fig. 4 that the slopes of OP curves, which represents the diversity gain of the system, does not depend on both  $N$  and  $M$ . Another important observation in Fig. 4 is that, when  $[N, M] = [1, 1]$ , the OPs of both TAS/SC and TAS/MRC schemes are similar. However, for other  $[N, M]$ , the OP of TAS/SC scheme is higher than that of TAS/MRC

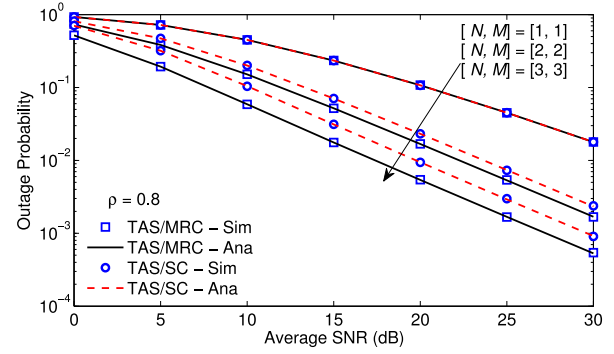


Fig. 4. Outage probabilities of TAS/MRC and TAS/SC schemes versus the average SNR for different  $[N, M]$  pairs.

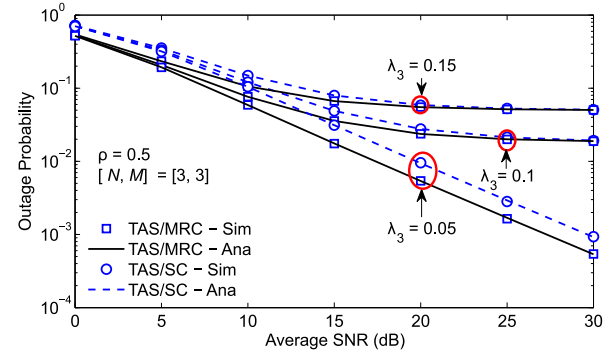


Fig. 5. Outage probabilities of TAS/MRC and TAS/SC schemes versus the average SNR for different average channel gain  $\lambda_3$  of self-interference channel.

scheme. This feature can be explained as follows. For TAS/MRC scheme, since the output is a weighted sum of all branches, the SNR at the output of signal combiner will be the summation of the SNR of each branch. Consequently, the average SNR increases linearly with the number of diversity branches  $M$ . In contrast, for TAS/SC scheme, the SNR at the output of signal combiner is the SNR of the branch with highest signal quality. Thus, the average SNR does not linearly increase with  $M$ . On the other hand, the summation of real numbers smaller than one is always greater than their product.

Fig. 5 illustrates the impact of SIC capability at FDR node on the OPs of TAS/SC and TAS/MRC schemes for different average channel gain  $\lambda_3$  of self-interference channel. We evaluate the OPs in three cases of  $\lambda_3$ , i.e.,  $\lambda_3 = [0.15, 0.1, 0.05]$ . As can be seen in Fig. 5, the SIC capability greatly determines the shape of OP curve. Specifically, when the RSI is large, e.g.,  $\lambda_3 = 0.15$ , the OP decreases slowly and goes to the outage floor quickly. For better SIC, e.g.,  $\lambda_3 = 0.05$ , the OP decreases faster and avoids the outage floor. Therefore, it is absolutely necessary to apply all techniques of SIC<sup>12</sup> into FD relay. Besides, we can see that the outage performance of TAS/MRC scheme is always better than that of TAS/SC scheme.

Fig. 6 depicts the impact of optimal time switching  $\alpha$  on the OP of TAS/SC scheme for three  $[N, M]$  pairs, i.e.,  $[N, M] = [1, 1]$ ,  $[N, M] = [1, 2]$ , and  $[N, M] = [2, 2]$ . The transmission

<sup>12</sup>SIC techniques include isolation, propagation domain, digital and analog cancellation.

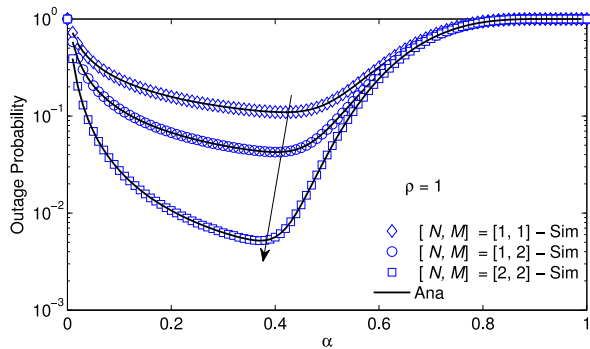


Fig. 6. Effect of  $\alpha$  on the outage probability of TAS/SC scheme for different  $[N, M]$  pairs.  $P_S = 20$  dB.

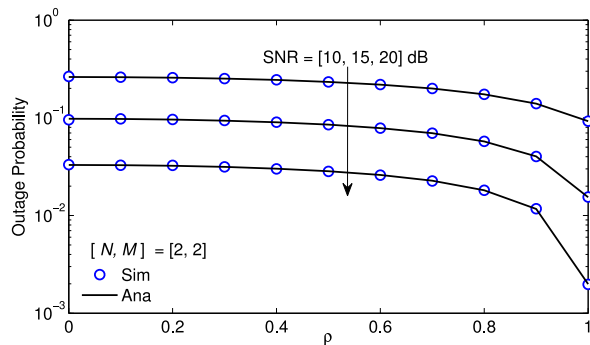


Fig. 7. Outage probability of TAS/SC scheme versus  $\rho$  for different average SNRs.  $N = 2, M = 2$ .

power of source is fixed at  $P_S = 20$  dB while  $\alpha$  continuously increases from 0 to 1. We can see that the optimal value of  $\alpha$  that minimizes the OP is different for each antenna configuration.<sup>13</sup> Moreover, when the number of antennas increases, the optimal value of  $\alpha$  reduces. Specifically, for  $[N, M] = [1, 1]$ , the optimal value of  $\alpha$  is larger than 0.4, but for  $[N, M] = [2, 2]$ , the optimal value of  $\alpha$  is less than 0.4. It is because the array gain is improved so that the relay node can transmit with lower power with the same required reliability, resulting in the reduction in  $\alpha$ .

Fig. 7 depicts the OP of TAS/SC scheme versus  $\rho$  for different average SNRs in dB. The number of antennas of S is  $N = 2$  and the number of antennas of D is  $M = 2$ . We can see that as  $\rho$  increases (i.e., the CSI from R to the antenna of S is more exact), the OP reduces. The improved CSI helps to select the best antenna to assist the source transmission. Fig. 7 also shows that when  $\rho < 0.8$ , the enhancement of outage performance is not significant as  $\rho$  increases. It is only remarkable when  $\rho$  is close to 1.

Fig. 8 presents the SEPs of TAS/MRC and TAS/SC schemes versus the average SNR in dB for different channel correlation

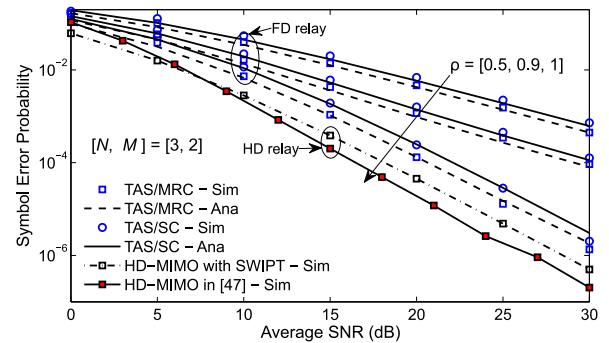


Fig. 8. Symbol error probability of TAS/SC scheme versus the average SNR in dB for different correlation coefficients  $\rho$ .

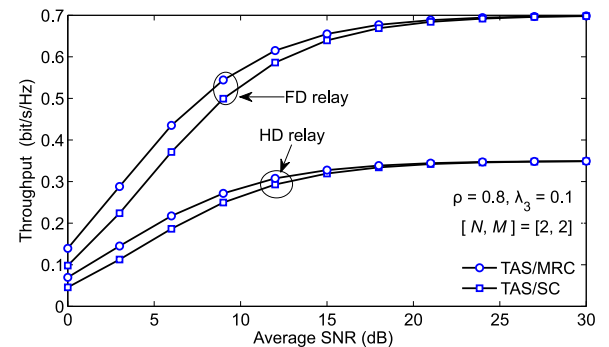


Fig. 9. Comparison between the throughputs of HDR and FDR systems versus SNR in dB,  $\alpha = 0.3$ .

coefficients  $\rho$ . We set  $[N, M] = [3, 2]$  to compare with the HD-MIMO system without SWIPT in [50]. Firstly, we see that increasing  $\rho$  enhances the SEP performance. Another important observation is that the difference in the diversity gains of partial correlation and full correlation is significant in moderate and high SNR regimes. The results show that both TAS/MRC and TAS/SC schemes have similar diversity orders, which are approximation to 2 in the case of perfect CSI ( $\rho = 1$ ) although we use a part of signal period for EH. The TAS/SC scheme is suggested as a good choice in practice because of its low implementation complexity. However, to reduce the energy harvesting time or transmission power while still ensure the system performance, TAS/MRC scheme should be used. Furthermore, we can see that, although  $\alpha = 3$ , the diversity gain of HD-MIMO system with SWIPT is not very significant compared to that of HD-MIMO system without SWIPT, i.e., the diversity gain is around 1.7 dB at  $SEP = 5 \times 10^{-5}$ .

Fig. 9 shows a comparison between the throughputs of FD-MIMO and HD-MIMO systems with SWIPT. From Fig. 9, we see that the throughput of FD-MIMO system is double compared to that of HD-MIMO system. This result is reasonable because the FD relay transmits and receives signals simultaneously while the HD relay receives and transmits signals in two separate time slots. As SNR increases, the throughputs of both FD-MIMO and HD-MIMO systems with SWIPT remain unchanged, indicating that the throughput cannot be improved by simply increasing the SNR of transmitted signal. Instead, it is determined by the data rate threshold,  $\mathcal{R}_{th} = 1$  bit/s/Hz.

<sup>13</sup>The optimization problem for minimizing the OP is expressed as

$$\begin{aligned} \alpha_{\text{opt}} &= \arg \min_{\alpha} \text{OP}(\alpha) \\ \text{subject to } & 0 < \alpha < 1 \end{aligned} \quad (48)$$

Using this optimization problem, it is very difficult to obtain the closed-form expression of  $\alpha_{\text{opt}}$ . Fortunately, we can numerically find  $\alpha_{\text{opt}}$  by using Matlab or Mathematica.

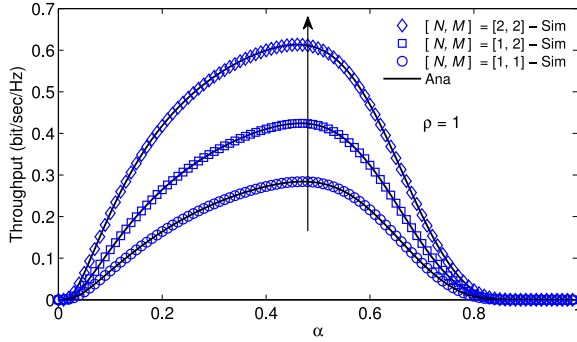


Fig. 10. Effect of  $\alpha$  on the system throughput of TAS/SC scheme for with different  $[N, M]$  pairs.  $P_S = 20$  dB,  $\rho = 1$ .

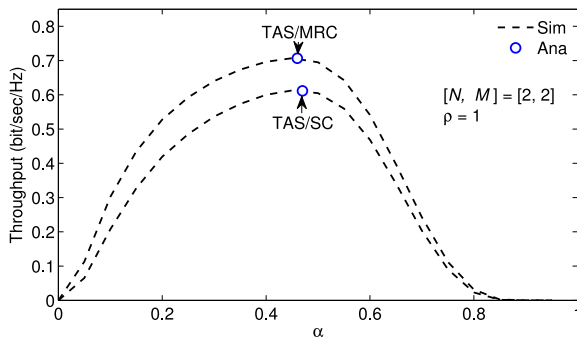


Fig. 11. Comparison between the throughput of TAS/SC and TAS/MRC schemes versus  $\alpha$ .  $N = M = 2$ ,  $P_S = 20$  dB,  $\rho = 1$ .

Fig. 10 plots the throughput of TAS/SC scheme versus the time switching ratio  $\alpha$  for different  $[N, M]$  pairs. We can see in Fig. 10 that for each  $[N, M]$  pair, there exists an optimal value of  $\alpha$  that maximizes the throughput. Specifically, as  $\alpha$  goes from 0 to 1, the system throughput increases from zero to the maximum value at which the value  $\alpha$  is optimal. Then, the throughput decreases from that maximum value to zero. Moreover, the throughput is increased with  $[N, M]$  but is inversely proportional to  $\alpha$  but larger  $\alpha$  reduces the effectiveness of the forwarding time as shown in (39).

Fig. 11 shows the throughputs of both TAS/SC and TAS/MRC schemes with the optimal value of  $\alpha$  is obtained in (42a). We can see that TAS/MRC scheme provides better throughput than TAS/SC scheme. Besides, the optimal values of  $\alpha$  corresponding to TAS/SC and TAS/MRC schemes are different. It is worth noticing that, the values of  $\alpha$  that minimizes OP (Fig. 6) and maximizes throughput (Figs. 10 and 11) are also different, i.e.,  $\alpha$  that maximizes throughput is larger than  $\alpha$  that minimizes OP. This reason behind this feature is that, the throughput is linearly proportional to the rate threshold while the OP is exponentially proportional to the rate threshold.

## VI. CONCLUSION

In this paper, we have proposed a MIMO-FDR system with SWIPT where multiple antennas are used at source and destination. We successfully derived the CDF of the SNR then used it to obtain the closed-form expressions of the OP, SEP, and throughput of the proposed MIMO-FDR system with SWIPT when TAS/SC and TAS/MRC schemes were used to select the transmit antenna under the condition of imperfect CSI. The validity of these mathematical expressions were confirmed by Monte-Carlo simulations. Numerical results show that better feedback knowledge of CSI improve the outage and SEP performance. Furthermore, when the number of antennas at source and destination  $[N, M] = 1$ , the OPs of both TAS/SC and TAS/MRC schemes are similar. However, as  $[N, M]$  increases, TAS/MRC scheme has lower OP than TAS/SC scheme. The throughput of TAS/MRC scheme is higher than that of TAS/SC scheme. The throughputs of both FD-MIMO and HD-MIMO systems increase with the SNR of transmitted signal and the number of antennas. Unfortunately, these throughputs cannot be improved further by simply increasing the SNR of transmitted signal but is determined by the data rate threshold. Lastly, the optimal time switching ratio  $\alpha$  that minimizes the OP is different for each  $[N, M]$  setting. When  $[N, M]$  increases, the optimal  $\alpha$  reduces. Moreover, the value of  $\alpha$  that maximizes throughput is larger than the value of  $\alpha$  that minimizes OP. Our proposed MIMO-FDR system with SWIPT is especially useful for unmanned aerial vehicle (UAV)-assisted relay systems because using multiple antenna at source and destination instead of the relay helps to reduce the hardware complexity, power consumption, and self-interference at the relaying UAV.

## APPENDIX A

The outage probability is the CDF of random variable  $\gamma$ , i.e.,  $OP = F_\gamma(\gamma_{th}) = \int_0^{\gamma_{th}} f_\gamma(\gamma) d\gamma$ . Hence, from (17), the CDF of the end-to-end SNR of the TAS/SC scheme is

$$F_{\gamma_{e2e}}^{TAS/SC}(\gamma) = 1 - \Psi(\Sigma) \left[ 1 - \exp\left(-\frac{1}{\phi\lambda_3\gamma}\right) \right] \times \sqrt{\frac{4ij\gamma\sigma_D^2}{\phi P_S \lambda_1 \Delta(\rho)\lambda_2}} \mathcal{K}_1 \left( \sqrt{\frac{4ij\gamma\sigma_D^2}{\phi P_S \lambda_1 \Delta(\rho)\lambda_2}} \right), \quad (49)$$

After having the CDF, by substituting (49) into (29), we get the symbol error probability of TAS/SC scheme as in (50), shown at the bottom of this page. For simplicity, we can rewrite (50) as

$$SEP_{TAS/SC} = \frac{a}{2} - [I_1 - I_2], \quad (51)$$

$$SEP = \frac{a\sqrt{b}}{2\sqrt{\pi}} \int_0^\infty \frac{e^{-b\gamma}}{\sqrt{\gamma}} \left[ 1 - \Psi(\Sigma) \left\{ 1 - \exp\left(-\frac{1}{\phi\lambda_3\gamma}\right) \right\} \sqrt{\frac{4ij\gamma\sigma_D^2}{\phi P_S \lambda_1 \Delta(\rho)\lambda_2}} \mathcal{K}_1 \left( \sqrt{\frac{4ij\gamma\sigma_D^2}{\phi P_S \lambda_1 \Delta(\rho)\lambda_2}} \right) \right] d\gamma \quad (50)$$

$$\begin{aligned}\mathcal{I}_1 &= \frac{a\sqrt{b}}{2\sqrt{\pi}}\Psi(\Sigma)\int_0^\infty \frac{e^{-b\gamma}}{\sqrt{\gamma}}\sqrt{\frac{4ij\gamma\sigma_D^2}{\phi P_S\lambda_1\Delta(\rho)\lambda_2}}\mathcal{K}_1\left(\sqrt{\frac{4ij\gamma\sigma_D^2}{\phi P_S\lambda_1\Delta(\rho)\lambda_2}}\right)d\gamma \\ &= \frac{a\sqrt{b}}{2\sqrt{\pi}}\Psi(\Sigma)\sqrt{\frac{4ij\sigma_D^2}{\phi P_S\lambda_1\Delta(\rho)\lambda_2}}\int_0^\infty e^{-b\gamma}\mathcal{K}_1\left(\sqrt{\frac{4ij\gamma\sigma_D^2}{\phi P_S\lambda_1\Delta(\rho)\lambda_2}}\right)d\gamma\end{aligned}\quad (52)$$

$$\mathcal{I}_2 = \frac{a\sqrt{b}}{2\sqrt{\pi}}\Psi(\Sigma)\int_0^\infty \frac{e^{-b\gamma}}{\sqrt{\gamma}}\exp\left(-\frac{1}{\phi\lambda_3\gamma}\right)\sqrt{\frac{4ij\gamma\sigma_D^2}{\phi P_S\lambda_1\Delta(\rho)\lambda_2}}\mathcal{K}_1\left(\sqrt{\frac{4ij\gamma\sigma_D^2}{\phi P_S\lambda_1\Delta(\rho)\lambda_2}}\right)d\gamma\quad (53)$$

$$\begin{aligned}\mathcal{I}_3 &= \frac{a\sqrt{b}}{2\sqrt{\pi}}\sum_{i=1}^N(-1)^{i-1}\binom{N}{i}\frac{2}{\Gamma(M)\lambda_2^M}\int_0^\infty \frac{e^{-b\gamma}}{\sqrt{\gamma}}\left(\frac{i\gamma\sigma_D^2\lambda_2}{\phi P_S\lambda_1\Delta(\rho)}\right)^{\frac{M}{2}}\mathcal{K}_M\left(\sqrt{\frac{4i\gamma\sigma_D^2}{\lambda_1\Delta(\rho)\lambda_2\phi P_S}}\right)d\gamma \\ &= \sum_{i=1}^N(-1)^{i-1}\binom{N}{i}\frac{2}{\Gamma(M)\lambda_2^M}\frac{a\sqrt{b}}{2\sqrt{\pi}}\left(\frac{i\sigma_D^2\lambda_2}{\phi P_S\lambda_1\Delta(\rho)}\right)^{\frac{M}{2}}\int_0^\infty \gamma^{\frac{M}{2}-\frac{1}{2}}e^{-b\gamma}\mathcal{K}_M\left(\sqrt{\frac{4i\gamma\sigma_D^2}{\lambda_1\Delta(\rho)\lambda_2\phi P_S}}\right)d\gamma\end{aligned}\quad (57)$$

$$\begin{aligned}\mathcal{I}_4 &= \frac{a\sqrt{b}}{2\sqrt{\pi}}\sum_{i=1}^N(-1)^{i-1}\binom{N}{i}\frac{2}{\Gamma(M)\lambda_2^M}\int_0^\infty \frac{e^{-b\gamma}}{\sqrt{\gamma}}\exp\left(-\frac{1}{\phi\lambda_3\gamma}\right)\left(\frac{i\gamma\sigma_D^2\lambda_2}{\phi P_S\lambda_1\Delta(\rho)}\right)^{\frac{M}{2}}\mathcal{K}_M\left(\sqrt{\frac{4i\gamma\sigma_D^2}{\lambda_1\Delta(\rho)\lambda_2\phi P_S}}\right)d\gamma \\ &= \sum_{i=1}^N(-1)^{i-1}\binom{N}{i}\frac{2}{\Gamma(M)\lambda_2^M}\frac{a\sqrt{b}}{2\sqrt{\pi}}\left(\frac{i\sigma_D^2\lambda_2}{\phi P_S\lambda_1\Delta(\rho)}\right)^{\frac{M}{2}}\int_0^\infty \gamma^{\frac{M}{2}-\frac{1}{2}}\exp\left(-\frac{1}{\phi\lambda_3\gamma}-b\gamma\right)\mathcal{K}_M\left(\sqrt{\frac{4i\gamma\sigma_D^2}{\lambda_1\Delta(\rho)\lambda_2\phi P_S}}\right)d\gamma\end{aligned}\quad (58)$$

where  $\frac{a\sqrt{b}}{2\sqrt{\pi}}\int_0^\infty \frac{e^{-b\gamma}}{\sqrt{\gamma}} = \frac{a}{2}$ , and  $\mathcal{I}_1$  and  $\mathcal{I}_2$  can be rewritten as in (52) and (53), shown at the top of this page.

Using [25, Eq. (6.614.5)] and after some manipulations on (52), we obtain  $\mathcal{I}_1$  as in (26).

When  $P_S$  is in high regime,  $\sqrt{\frac{4ij\gamma\sigma_D^2}{\phi P_S\lambda_1\Delta(\rho)\lambda_2}}$  is small enough. Then, by using the approximation of Bessel function [51, Eq. (9.6.9)] as  $\mathcal{K}_1(z) \approx \frac{1}{z}$ , we can rewrite  $\mathcal{I}_2$  as

$$\mathcal{I}_2 = \frac{a\sqrt{b}}{2\sqrt{\pi}}\Psi(\Sigma)\int_0^\infty x^{-\frac{1}{2}}\exp\left(-b\gamma - \frac{1}{\phi\lambda_3\gamma}\right)d\gamma.\quad (54)$$

From [25, (3.471.9)] and after some manipulations, we obtain  $\mathcal{I}_2$  as in (27). The proof of Theorem 1 is completed.

## APPENDIX B

Similar to the proof of Theorem 1, from (30) we present the CDF of the end-to-end SNR of TAS/MRC scheme with respect to  $\gamma$ ,  $F_{\gamma_{e2e}}^{\text{MRC}}(\gamma)$ , as

$$\begin{aligned}F_{\gamma_{e2e}}^{\text{MRC}}(\gamma) &= 1 - \sum_{i=1}^N(-1)^{i-1}\binom{N}{i}\left[1 - \exp\left(-\frac{1}{\phi\lambda_3\gamma}\right)\right] \\ &\times \frac{2}{\Gamma(M)\lambda_2^M}\left(\frac{i\gamma\sigma_D^2\lambda_2}{\phi P_S\lambda_1\Delta(\rho)}\right)^{\frac{M}{2}}\mathcal{K}_M\left(\sqrt{\frac{4i\gamma\sigma_D^2}{\lambda_1\Delta(\rho)\lambda_2\phi P_S}}\right).\end{aligned}\quad (55)$$

By substituting (55) into (29), we have the SEP of TAS/MRC scheme as in (56).

$$\text{SEP}_{\text{TAS/MRC}} = \frac{a}{2} - [\mathcal{I}_3 - \mathcal{I}_4],\quad (56)$$

where  $\mathcal{I}_3$  and  $\mathcal{I}_4$  are presented in (57) and (58), shown at the top of this page, respectively.

Using [25, Eq. (6.643.3)], after some manipulations on (57), we obtain the closed-form expression of  $\mathcal{I}_3$  as in (37).

To calculate the integration in (58), we use the approximation of Bessel function  $\mathcal{K}_n(z) = \frac{(n-1)!}{2}\left(\frac{z}{2}\right)^{-n}$  provided in [51, Eq. (9.6.9)]. After some manipulations, we have

$$\mathcal{I}_4 = \sum_{i=1}^N(-1)^{i-1}\binom{N}{i}\frac{a\sqrt{b}}{\sqrt{\pi}}\left(\frac{1}{2}\right)^{\frac{M}{2}}\int_0^\infty \gamma^{\frac{1}{2}-1}e^{-\frac{1}{\phi\lambda_3\gamma}-b\gamma}d\gamma.\quad (59)$$

Finally, applying [25, Eq. (3.471.9)] and after some manipulations, we obtain  $\mathcal{I}_4$  as in (38). The proof of Theorem 2 is completed.

## REFERENCES

- [1] I. Randrianantenaina, H. ElSawy, H. Dahrouj, M. Kaneko, and M. Alouini, "Uplink power control and ergodic rate characterization in FD cellular networks: A stochastic geometry approach," *IEEE Trans. Commun.*, vol. 18, no. 4, pp. 2093–2110, Apr. 2019.
- [2] J. Huang and H. Gharavi, "Performance analysis of relay-based two-way D2D communications with network coding," *IEEE Trans. Veh. Technol.*, vol. 67, no. 7, pp. 6642–6646, Jul. 2018.

- [3] J. Huang, Y. Liao, C.-C. Xing, and Z. Chang, "Multi-hop D2D communications with network coding: From a performance perspective," *IEEE Trans. Veh. Technol.*, vol. 68, no. 3, pp. 2270–2282, Mar. 2019.
- [4] Y. Wang, Y. Xu, N. Li, W. Xie, K. Xu, and X. Xia, "Relay selection of full-duplex decode-and-forward relaying over Nakagami- $m$  fading channels," *IET Commun.*, vol. 10, no. 2, pp. 170–179, Mar. 2016.
- [5] I. Krikidis, G. Zheng, and B. Ottersten, "Harvest-use cooperative networks with half/full-duplex relaying," in *Proc. Wireless Commun. Netw. Conf.*, 2013, pp. 4256–4260.
- [6] M. Mohammadi, H. A. Suraweera, Y. Cao, I. Krikidis, and C. Tellambura, "Full-duplex radio for uplink/downlink wireless access with spatially random nodes," *IEEE Trans. Commun.*, vol. 63, no. 12, pp. 5250–5266, Dec. 2015.
- [7] T. Riihonen, S. Werner, and R. Wichman, "Mitigation of loopback self-interference in full-duplex MIMO relays," *IEEE Trans. Signal Process.*, vol. 59, no. 12, pp. 5983–5993, Dec. 2011.
- [8] M. Duarte, "Full-duplex wireless: Design, implementation and characterization," Ph.D. dissertation, Dept. Elect. Comput. Eng., Rice University, Houston, TX, USA, 2012.
- [9] K. David and H. Berndt, "6G vision and requirements: Is there any need for beyond 5G?," *IEEE Veh. Technol. Mag.*, vol. 13, no. 3, pp. 72–80, Sep. 2018.
- [10] T. M. Hoang, N. T. Tan, N. B. Cao, and L. T. Dung, "Outage probability of MIMO relaying full-duplex system with wireless information and power transfer," in *Proc. Conf. IEEE Inf. Commun. Technol.*, Nov. 2017, pp. 1–6.
- [11] T. M. Hoang, N. T. Tan, N. H. Hoang, and P. T. Hiep, "Performance analysis of decode-and-forward partial relay selection in NOMA systems with RF energy harvesting," *Wireless Netw.*, vol. 25, pp. 4585–4595, 2019.
- [12] T. M. Hoang, B. C. Nguyen, P. T. Tran, and L. T. Dung, "Outage analysis of RF energy harvesting cooperative communication systems over Nakagami- $m$  fading channels with integer and non-integer  $m$ ," *IEEE Trans. Veh. Technol.*, vol. 69, no. 3, pp. 2785–2801, Mar. 2020.
- [13] Ö. T. Demir and T. E. Tuncer, "Robust optimum and near-optimum beamformers for decode-and-forward full-duplex multi-antenna relay with self-energy recycling," *IEEE Trans. Wireless Commun.*, vol. 18, no. 3, pp. 1566–1580, Mar. 2019.
- [14] J. Huang, Y. Zhou, Z. Ning, and H. Gharavi, "Wireless power transfer and energy harvesting: Current status and future prospects," *IEEE Trans. Wireless Commun.*, vol. 26, no. 4, pp. 163–169, Aug. 2019.
- [15] M. Ju, K.-M. Kang, K.-S. Hwang, and C. Jeong, "Maximum transmission rate of PSR/TSR protocols in wireless energy harvesting DF-based relay networks," *IEEE J. Sel. Areas Commun.*, vol. 33, no. 12, pp. 2701–2717, Sep. 2015.
- [16] R. Zhang and C. K. Ho, "MIMO broadcasting for simultaneous wireless information and power transfer," *IEEE Trans. Commun.*, vol. 12, no. 5, pp. 1989–2001, May 2013.
- [17] C. Song and Y. Jeon, "Weighted MMSE precoder designs for sum-utility maximization in multi-user SWIPT network-MIMO with per-BS power constraints," *IEEE Trans. Veh. Technol.*, vol. 67, no. 3, pp. 2809–2813, Mar. 2018.
- [18] M.-M. Zhao, Y. Cai, Q. Shi, M. Hong, and B. Champagne, "Joint transceiver designs for full-duplex  $k$ -pair MIMO interference channel with SWIPT," *IEEE Trans. Commun.*, vol. 65, no. 2, pp. 890–905, 2016.
- [19] I. Pehlivan and S. C. Ergen, "Scheduling of energy harvesting for MIMO wireless powered communication networks," *IEEE Commun. Lett.*, vol. 23, no. 1, pp. 152–155, Jan. 2019.
- [20] A. Almradi and P. Xiao, "Energy beamforming for MIMO WIPT relaying with arbitrary correlation," *IEEE Access*, vol. 6, pp. 849–862, 2018.
- [21] T. M. Hoang, X. N. Tran, N. Thanh, and L. T. Dung, "Performance analysis of MIMO SWIPT relay network with imperfect CSI," *Mobile Netw. Appl.*, vol. 24, pp. 630–642, 2019.
- [22] M. Mohammadi, B. K. Chalise, H. A. Suraweera, C. Zhong, G. Zheng, and I. Krikidis, "Throughput analysis and optimization of wireless-powered multiple antenna full-duplex relay systems," *IEEE Trans. Commun.*, vol. 64, no. 4, pp. 1769–1785, Apr. 2016.
- [23] R. Zhao, H. Lin, Y.-C. He, D.-H. Chen, Y. Huang, and L. Yang, "Secrecy performance of transmit antenna selection for MIMO relay systems with outdated CSI," *IEEE Trans. Commun.*, vol. 66, no. 2, pp. 546–559, 2018.
- [24] M. Toka and O. Kucur, "Outage analysis of TAS/MRC in dual hop full-duplex MIMO relay networks with co-channel interferences," *AEU-Int. J. Electron. Commun.*, vol. 77, pp. 82–90, 2017.
- [25] D. Zwillinger, *Table of Integrals, Series, and Products*. Cambridge, MA, USA: Elsevier, 2014.
- [26] D. Bharadia, E. McMillin, and S. Katti, "Full duplex radios," *Proc. ACM SIGCOMM*, vol. 43, no. 4, pp. 375–386, Aug. 2013.
- [27] A. A. Nasir, X. Zhou, S. Durrani, and R. A. Kennedy, "Relaying protocols for wireless energy harvesting and information processing," *IEEE Trans. Wireless Commun.*, vol. 12, no. 7, pp. 3622–3636, Jul. 2013.
- [28] X. Lu, P. Wang, D. Niyato, D. I. Kim, and Z. Han, "Wireless networks with RF energy harvesting: A contemporary survey," *IEEE Commun. Tut.*, vol. 17, no. 2, pp. 757–789, Mar. 2015.
- [29] J. Yuan, Z. Chen, B. Vucetic, and W. Firmanto, "Performance and design of space-time coding in fading channels," *IEEE Trans. Commun.*, vol. 51, no. 12, pp. 1991–1996, Dec. 2003.
- [30] Y. Zeng, Q. Wu, and R. Zhang, "Accessing from the sky: A tutorial on UAV communications for 5G and beyond," *Proc. IEEE*, vol. 107, no. 12, pp. 2327–2375, 2019.
- [31] J. Zhang and G. Pan, "Outage analysis of wireless-powered relaying MIMO systems with non-linear energy harvesters and imperfect CSI," *IEEE Access*, vol. 4, pp. 7046–7053, Oct. 2016.
- [32] R. M. Radaydeh, "Impact of delayed arbitrary transmit antenna selection on the performance of rectangular QAM with receive MRC in fading channels," *IEEE Commun. Lett.*, vol. 13, no. 6, pp. 390–392, Jun. 2009.
- [33] J. Xiong, Y. Tang, D. Ma, P. Xiao, and K.-K. Wong, "Secrecy performance analysis for TAS-MRC system with imperfect feedback," *IEEE Trans. Inf. Forensics Secur.*, vol. 10, no. 8, pp. 1617–1629, Apr. 2015.
- [34] H. A. Suraweera, P. J. Smith, and M. Shafi, "Capacity limits and performance analysis of cognitive radio with imperfect channel knowledge," *IEEE Trans. Veh. Commun.*, vol. 59, no. 4, pp. 1811–1822, Feb. 2010.
- [35] K. S. Ahn and J. R. W. Heath, "Performance analysis of maximum ratio combining with imperfect channel estimation in the presence of cochannel interferences," *IEEE Trans. Wireless Commun.*, vol. 8, no. 3, pp. 1080–1085, Mar. 2009.
- [36] H. A. Suraweera, M. Soysa, C. Tellambura, and H. K. Garg, "Performance analysis of partial relay selection with feedback delay," *IEEE Signal Process. Lett.*, vol. 17, no. 6, pp. 531–534, 2010.
- [37] Q. N. Le, V. N. Q. Bao, and B. An, "Full-duplex distributed switch-and-stay energy harvesting selection relaying networks with imperfect CSI: Design and outage analysis," *J. Commun. Netw.*, vol. 20, no. 1, pp. 29–46, 2018.
- [38] H. H. M. Tam, H. D. Tuan, A. A. Nasir, T. Q. Duong, and H. V. Poor, "MIMO energy harvesting in full-duplex multi-user networks," *IEEE Trans. Commun.*, vol. 16, no. 5, pp. 3282–3297, May 2017.
- [39] C. Zhong, H. A. Suraweera, G. Zheng, I. Krikidis, and Z. Zhang, "Wireless information and power transfer with full duplex relaying," *IEEE Trans. Commun.*, vol. 62, no. 10, pp. 3447–3461, Oct. 2014.
- [40] D. C. Gonzalez, D. B. Costa, and J. C. S. S. Filho, "Distributed TAS/MRC and TAS/SC schemes for fixed-gain AF systems with multiantenna relay: Outage performance," *IEEE Trans. Wireless Commun.*, vol. 15, no. 6, pp. 4380–4392, 2016.
- [41] Y. Chen, "Energy-harvesting af relaying in the presence of interference and nakagami-fading," *IEEE Trans. Commun.*, vol. 15, no. 2, pp. 1008–1017, Feb. 2016.
- [42] A. Papoulis and S. U. Pillai, *Probability, Random Variables, and Stochastic Processes*. New York, NY, USA: Tata McGraw-Hill Education, 2017.
- [43] Y. Chen and C. Tellambura, "Distribution functions of selection combiner output in equally correlated rayleigh, Rician, and Nakagami- $m$  fading channels," *IEEE Trans. Wireless Commun.*, vol. 52, no. 11, pp. 1948–1956, Nov. 2004.
- [44] M. K. Simon and M.-S. Alouini, *Digital Communication Over Generalized Fading Channels: A Unified Approach to Performance Analysis*. Hoboken, NJ, USA: John Wiley & Son, 2004.
- [45] A. Bletsas, H. Shin, and M. Z. Win, "Cooperative communications with outage-optimal opportunistic relaying," *IEEE Trans. Wireless Commun.*, vol. 6, no. 9, pp. 3450–3460, Sep. 2007.
- [46] A. Goldsmith, *Wireless Communications*. Cambridge Univ. Press, UK: Cambridge, 2005.
- [47] R. M. Corless, G. H. Gonnet, D. E. Hare, D. J. Jeffrey, and D. E. Knuth, "On the LambertW function," *Adv. Comput. Math.*, vol. 5, no. 1, pp. 329–359, 1996.
- [48] S. Sesia, I. Toufik, and M. Baker, *LTE-The UMTS Long Term Evolution: From Theory to Practice*. Hoboken, NJ, USA: John Wiley & Sons, 2011.
- [49] X. Li, M. Liu, C. Deng, P. T. Mathiopoulos, Z. Ding, and Y. Liu, "Full-duplex cooperative NOMA relaying systems with I/q imbalance and imperfect SIC," *IEEE Commun. Lett.*, vol. 9, no. 1, pp. 17–20, Jan. 2020.
- [50] A. Yilmaz and O. Kucur, "Performance of transmit antenna selection and maximal-ratio combining in dual HOP amplify-and-forward relay network over Nakagami- $m$  fading channels," *Wireless Pers. Commun.*, vol. 67, no. 3, pp. 485–503, 2012.
- [51] M. Abramowitz, *Handbook of Mathematical Functions: With Formulas, Graphs, and Mathematical Tables*. Mineola, NY, USA: Dover Publications, 1974.



**Tran Manh Hoang** received the B.S. degree in communication command from Telecommunications University, Ministry of Defense, Nha Trang, Vietnam, in 2002, the B.Eng. degree in electrical engineering from Le Quy Don Technical University, Ha Noi, Vietnam, in 2006, the M.Eng. degree in electronics engineering from the Posts and Telecommunications Institute of Technology, Ho Chi Minh City, Vietnam, in 2013, and the Ph.D. degree from Le Quy Don Technical University, Hanoi, Vietnam, in 2018. He is currently a Lecturer with Telecommunications University, Nha Trang, Vietnam. His research interests include energy harvesting, non-orthogonal multiple access, and signal processing for wireless cooperative communications.



**Ba Cao Nguyen** received the B.S. degree from Telecommunication University, Nha Trang, Vietnam, in 2006, and the M.S. degree from the Posts and Telecommunications Institute of Technology (VNPT), Ho Chi Minh City, Vietnam, in 2011. He received the Ph.D. degree from Le Quy Don Technical University, Hanoi, Vietnam. He is currently a Lecturer with Telecommunications University, Nha Trang, Vietnam. His research interests include energy harvesting, full-duplex, spatial modulation, NOMA, MIMO, and cooperative communication.



**Xuan Nam Tran** (Member, IEEE) received M.E. degree in telecommunications engineering from the University of Technology Sydney, Australia in 1998, and D.Eng. in electronic engineering from The University of Electro-Communications, Japan, in 2003. He is currently a Full Professor and Head of a strong research group on advanced wireless communications, Le Quy Don Technical University. From November 2003 to March 2006, he was a Research Associate with the Information and Communication Systems Group, Department of Information

and Communication Engineering, The University of Electro-Communications, Tokyo, Japan. His research interests include the areas of space-time signal processing for communications such as adaptive antennas, space-time coding, MIMO, spatial modulation and cooperative communications. He was the recipient of the 2003 IEEE AP-S Japan Chapter Young Engineer Award, and a Co-Recipient of two Best Papers from The 2012 International Conference on Advanced Technologies for Communications and The 2014 National Conference on Electronics, Communications and Information Technology. He is the Founding Chair and currently the Chapter Chair of the Vietnam Chapter of IEEE Communications Society. He is a member of IEICE and the Radio-Electronics Association of Vietnam (REV).



**Le The Dung** (Member, IEEE) received the B.S. degree in electronics and telecommunication engineering from the Ho Chi Minh City University of Technology, Ho Chi Minh City, Vietnam, in 2008 and the M.S. and Ph.D. degrees in electronics and computer engineering from Hongik University, Seoul, South Korea, in 2012 and 2016, respectively. From 2007 to 2010, he was with Signet Design Solutions Vietnam as a Hardware Design Engineer. He has been with Chungbuk National University as a Postdoctoral Research Fellow from May 2016. He has authored or

coauthored more than 50 papers in referred international journals and conferences. His major research interests include routing protocols, network coding, network stability analysis and optimization in mobile ad-hoc networks, cognitive radio ad-hoc networks, and visible light communication networks. He was the recipient of the IEEE IS3C2016 Best Paper Award.